

# Cellular Entry of G3.5 Poly (amido amine) Dendrimers by Clathrin- and Dynamin-Dependent Endocytosis Promotes Tight Junctional Opening in Intestinal Epithelia

Deborah S. Goldberg · Hamidreza Ghandehari · Peter W. Swaan

Received: 28 February 2010 / Accepted: 6 April 2010 / Published online: 22 April 2010  
© Springer Science+Business Media, LLC 2010

## ABSTRACT

**Purpose** This study investigates the mechanisms of G3.5 poly (amido amine) dendrimer cellular uptake, intracellular trafficking, transepithelial transport and tight junction modulation in Caco-2 cells in the context of oral drug delivery.

**Methods** Chemical inhibitors blocking clathrin-, caveolin- and dynamin-dependent endocytosis pathways were used to investigate the mechanisms of dendrimer cellular uptake and transport across Caco-2 cells using flow cytometry and confocal microscopy.

**Results** Dendrimer cellular uptake was found to be dynamin-dependent and was reduced by both clathrin and caveolin endocytosis inhibitors, while transepithelial transport was only dependent on dynamin- and clathrin-mediated endocytosis. Dendrimers were quickly trafficked to the lysosomes after 15 min of incubation and showed increased endosomal

accumulation at later time points, suggesting saturation of this pathway. Dendrimers were unable to open tight junctions in cell monolayers treated with dynasore, a selective inhibitor of dynamin, confirming that dendrimer internalization promotes tight junction modulation.

**Conclusion** G3.5 PAMAM dendrimers take advantage of several receptor-mediated endocytosis pathways for cellular entry in Caco-2 cells. Dendrimer internalization by dynamin-dependent mechanisms promotes tight junction opening, suggesting that dendrimers act on intracellular cytoskeletal proteins to modulate tight junctions, thus catalyzing their own transport via the paracellular route.

**KEY WORDS** endocytosis · oral drug delivery · PAMAM dendrimers · tight junctions · transport

## ABBREVIATIONS

AF	alexa fluor
BSA	bovine serum albumin
CH	carbohydrazide
DAPI	4',6-diamidino-2-phenylindole
DI	deionized
DMEM	Dulbecco's modified eagle's medium
DPBS	Dulbecco's phosphate-buffered saline
DYN	Dynasore
EDC	1-Ethyl-3-(3-dimethylaminopropyl)-carbodiimide
EDTA	ethylenediamine tetraacetic acid
EEA-1	early endosome antigen-1
FBS	fetal bovine serum
FIL	filipin
G	generation
GEN	genistein
HBSS	Hank's balanced salt solution
HEPES	N-(2-hydroxyethyl)piperazine-N'-179 (2 ethanesulfonic acid) hemisodium salt
LAMP-1	lysosome-associated membrane protein 1

D. S. Goldberg · H. Ghandehari · P. W. Swaan  
Fischell Department of Bioengineering, University of Maryland  
College Park, Maryland 20742, USA

D. S. Goldberg · P. W. Swaan  
Center for Nanomedicine and Cellular Delivery  
University of Maryland  
Baltimore, Maryland 21201, USA

P. W. Swaan  
Department of Pharmaceutical Sciences, University of Maryland  
Baltimore, Maryland 21201, USA

H. Ghandehari  
Departments of Pharmaceutics and Pharmaceutical Chemistry  
and Bioengineering, University of Utah  
Salt Lake City, Utah 84108, USA

H. Ghandehari (✉)  
Utah Center for Nanomedicine, Nano Institute of Utah  
University of Utah  
Salt Lake City, Utah 84108, USA  
e-mail: hamid.ghandehari@pharm.utah.edu

LY	lucifer yellow CH
MDC	monodansyl cadaverine
MWCO	molecular weight cutoff
OG	Oregon green
PAMAM	poly (amido amine)
PAO	phenylarsine oxide
PBS	phosphate-buffered saline
PD10	protein desalting column
TEER	transepithelial electrical resistance
TJ	tight junction
WST-1	water-soluble tetrazolium salt

## INTRODUCTION

Poly (amido amine) (PAMAM) dendrimers have shown promise as drug delivery carriers due to their unique physical properties, including nanoscale size and near monodispersity (1). With each increase in dendrimer generation, the diameter increases linearly while the number of surface groups increases exponentially, creating high density surface groups that can be conjugated to drugs, imaging agents and targeting moieties, making them versatile multifunctional nanocarriers (2, 3). Reports from our laboratory (4–7) and others (8–11) have demonstrated that PAMAM dendrimers in a specified size and charge window can effectively cross the epithelial layer of the gut, showing potential as oral drug delivery carriers. Conjugation or complexation of therapeutics with poor solubility and low permeability (e.g. Biopharmaceutics Classification System Class 3 and 4 compounds) to water-soluble dendrimers that can permeate the epithelial layer of the gut has the potential to render these drugs orally bioavailable (12–14). Oral drug administration has many advantages, including the convenience of at-home administration, reduction of direct and indirect costs, and a more flexible dosing regimen, resulting in higher patient compliance and a lower burden on hospitals and the healthcare system (15).

PAMAM dendrimers are known to cross the epithelial barrier by a combination of transcellular and paracellular mechanisms. Transport of cationic dendrimers has been found to be energy dependent and is reduced in the presence of endocytosis inhibitors, signifying the importance of endocytosis in dendrimer transport (16). In addition, dendrimers were found to colocalize with clathrin and early endosome markers, suggesting the involvement of clathrin-mediated endocytosis in dendrimer internalization (17). Dendrimers have also been reported to interact with tight junctions, transiently opening them to allow for paracellular transport (4). While there has been significant progress in understanding the mechanisms by which dendrimers enter cells and are transported across the epithelial barrier, several important questions remain to

be addressed. In particular, the contributions of different endocytosis pathways to dendrimer cellular uptake and transcytosis and the specific mechanisms by which dendrimers open tight junctions have yet to be elucidated. Additionally, the majority of mechanistic studies to date have focused on cationic dendrimers, which are promising due to their high transport rates, but are limited by their significant cytotoxicity. Anionic dendrimers show comparably low cytotoxicity but still appreciable transport rates, making them well suited for oral delivery (18, 19).

In this study, we investigated the mechanisms of cellular uptake, transepithelial transport and tight junctional modulation of anionic G3.5 PAMAM dendrimers by examining the impact of endocytosis inhibitors on dendrimer interaction with Caco-2 cells and differentiated Caco-2 monolayers. In addition, we monitored the intracellular trafficking of dendrimers from endosomes to lysosomes over time. Knowledge of the specific pathways of endocytosis, intracellular trafficking and transepithelial transport will aid in rational design of dendrimers for oral delivery.

## MATERIALS AND METHODS

### Materials

G3.5 PAMAM dendrimers (reported molecular weight = 12,931), lucifer yellow CH dipotassium salt, oregon green carboxylic acid succinimidyl ester, monodansyl cadaverine, phenylarsine oxide, filipin, genistein and dynasore were purchased from Sigma Aldrich (St. Louis, MO). Superose 12 HR 10/300 GL column was obtained from Amersham Pharmacia Biotech (Piscataway, NJ) and WST-1 cell proliferation reagent from Roche Applied Sciences (Indianapolis, IN). Caco-2 cells were obtained from American Type Cell Culture (Rockville, MD).

### Synthesis of G3.5-OG

Purified G3.5 PAMAM dendrimers were first modified with pendant primary amine groups to facilitate Oregon Green (OG) labeling (18). Fifty mg dendrimer was dissolved in deionized (DI) water to a final concentration of 10 mg/ml, and the pH was adjusted to 6.5. 1-Ethyl-3-(3-dimethylaminopropyl)-carbodiimide (EDC) was added at a 5:1 molar ratio to the dendrimer and stirred for 30 min at room temperature, after which ethylene diamine was added at a 5:1 molar ratio and stirred for 4 h at room temperature. The sample volume was reduced to 1 ml by rotoevaporation of water and then run through a PD10 column followed by purification with an amicon centrifugal filter (MWCO 4000) to remove the EDC and ethylene diamine. Size exclusion chromatography was

used to confirm the absence of low molecular weight impurities. The number of amines per dendrimer was determined to be 2.5 by the ninhydrin assay. Ten mg of amine-modified dendrimer was dissolved in 25 ml of DI water, and 1 equivalent of Oregon green carboxylic succinimidyl ester per dendrimer was added and stirred for 30 min. The water was removed by rotoevaporation, and the product was redissolved in methanol and added dropwise to diethyl ether to precipitate the G3.5-OG conjugate. The solution was centrifuged and the ether decanted, and then the precipitate was dried overnight under vacuum. The precipitate was then redissolved in 1 ml of water and passed through a PD10 column to remove unreacted OG. Size exclusion chromatography was used to confirm the absence of free dye. OG content was determined, by a fluorescence standard curve ( $\lambda_{\text{excitation}} = 485 \text{ nm}$ ,  $\lambda_{\text{emission}} = 535 \text{ nm}$ ), to be 0.75 molecules of OG per dendrimer on average.

### Caco-2 Cell Culture

Caco-2 cells (passages 30–45) were grown at 37°C in an atmosphere of 95% relative humidity and 5% CO<sub>2</sub>. Cells were maintained in T-75 flasks using Dulbecco's Modified Eagle's Medium (DMEM) supplemented with 10% fetal bovine serum (FBS), 1% non-essential amino acids, 10,000 units/mL penicillin, 10,000 µg/mL streptomycin and 25 µg/mL amphotericin B. Media was changed every other day, and cells were passaged at 80–90% confluence using a 0.25% trypsin/ethylenediamine tetraacetic acid (EDTA) solution. Incubation buffer used in assays consisted of Hank's balanced salt solution (HBSS), supplemented with 1.0 mM N-(2-hydroxyethyl)piperazine-N'-179 (2 ethanesulfonic acid) hemisodium salt (HEPES) buffer (pH 7.4).

### Cytotoxicity of Endocytosis Inhibitors

Potential short-term cytotoxicity of endocytosis inhibitors was assessed in Caco-2 cells to ensure cell viability during uptake and transport assays. Chemical inhibitors were prepared at a range of concentrations known to reduce clathrin-mediated endocytosis (phenylarsine oxide (1–20 µM), monodansyl cadaverine (100–300 µM)), caveolin-mediated endocytosis (filipin (1–4 µM), genistein (100–300 µM)) or dynamin-dependent endocytosis (dynasore (40–80 µM)) (20–22). Cytotoxicity of the inhibitors was assessed by the water-soluble tetrazolium salt (WST-1) assay. Caco-2 cells were seeded at 50,000 cells per well in 96-well cell culture plates (Corning, Corning, NY) and maintained at 37°C, 95% relative humidity and 5% CO<sub>2</sub> for 48 h. Cells were washed with warm HBSS buffer and incubated for 2 h with 100 µL of varying concentrations of endocytosis inhibitors. After 2 h, the inhibitor solutions were removed, and the cells were washed with warm HBSS

buffer. Ten µL WST-1 cell proliferation reagent in 100 µL of HBSS buffer was added to each well and incubated for 4 h at 37°C. Absorbance at 460 nm and background at 600 nm were measured using a SpectraMax 384 plate reader (Molecular Devices, Sunnyvale, CA). HBSS was used as a negative control for 100% cell viability. Cytotoxicity of inhibitor concentration was assessed in four replicates. Cell viability of greater than 85% was classified as acceptable for uptake and transport assays.

### Cellular Uptake

Cellular uptake of G3.5-OG dendrimers was determined in the presence and absence of endocytosis inhibitors. Inhibitors were used at concentrations that showed a minimum of 85% cell viability during the 2 h assay period (Table I). Caco-2 cells were seeded at 300,000 cells per well in 12-well plates (Corning, Corning, NY) and maintained for 48 h at 37°C, 95% relative humidity and 5% CO<sub>2</sub>. Cells were washed with HBSS and pretreated with endocytosis inhibitors or HBSS for 1 h at 37°C. Endocytosis inhibitors were removed, and 25 µM G3.5-OG, 5 µM Transferrin-AF488 (Molecular Probes, Carlsbad, CA) or 5 µM Cholera Toxin B-AF488 (Molecular Probes, Carlsbad, CA) was added in the presence of endocytosis inhibitor solutions or HBSS for 1 h at 37°C. Cells were washed once with cold HBSS, trypsinized for 5 min and then complete cell culture medium was added to halt the trypsinization process. The cells were removed from plates, collected in microcentrifuge tubes and centrifuged for 5 min at 1,000 rpm, after which the supernatant was removed. The cells were washed with PBS and finally fixed in 1% paraformaldehyde in PBS at a final concentration of 500,000 cells/ml. Flow cytometry was used to assess cellular fluorescence using a BD LSR II flow cytometer (Becton Dickinson, Franklin Lakes, NJ) with a 530/30 bandpass filter. Twenty-five-thousand to forty-five-thousand events were collected per sample. Percent uptake was determined for two

**Table I** Endocytosis Inhibitor Concentration and % Cell Viability in Caco-2 Cells. Results are Reported as Mean  $\pm$  Standard Deviation with  $n = 4$

Endocytosis inhibitors		Concentration (µM)	% Cell viability
Clathrin Inhibiting	Phenylarsine Oxide (PAO)	1	90.0 $\pm$ 5.7%
	Monodansyl Cadaverine (MDC)	300	92.7 $\pm$ 3.4%
Caveolin Inhibiting	Filipin (FIL)	4	95.9 $\pm$ 2.7%
	Genistein (GEN)	100	86.7 $\pm$ 2.9%
Dynamin Inhibiting	Dynasore (DYN)	50	106.1 $\pm$ 5.0%

different cell populations by the shift in mean fluorescence in the presence of endocytosis inhibitors compared to HBSS control.

### Colocalization and Intracellular Trafficking

Caco-2 cells were seeded at 40,000 cells/cm<sup>2</sup> on collagen-coated 8-chamber slides. Slides were used when cells were 90% confluent, typically 4–5 days after seeding. Cells were washed with DPBS and then incubated in DPBS for 30 min at 37°C. Cells were treated with G3.5-OG (1 μM) or Transferrin-AF488 (250 μg/ml) for 30 min at 4°C to allow for attachment but not internalization (pulse). Subsequently, the cells were washed three times with ice-cold DPBS to remove unbound ligand and incubated with warm DPBS at 37°C for 5, 15, or 30 min (chase), after which they were fixed with 4% paraformaldehyde, 4% sucrose in DPBS for 20 min. All subsequent steps were carried out at room temperature. The cells were washed twice with 25 mM glycine and then once with DPBS, permeabilized with 1% Triton-X 100 in blocking solution (3% Bovine Serum Albumin (BSA)/DPBS) and then incubated with blocking solution to prevent non-specific binding. Primary antibodies for early endosomes (rabbit polyclonal early endosome antigen-1 (EEA-1)) and lysosomes (rabbit polyclonal lysosome-associated membrane protein 1 (LAMP-1)) (Molecular Probes, Carlsbad, CA) were added to separate chambers and incubated for 1 h. The antibodies were removed, cells were washed three times with blocking solution and Alexa Fluor-568 goat anti-rabbit IgG (Molecular Probes, Carlsbad, CA) was added at 1:400 in blocking solution for 1 h. The cells were then washed three times with DPBS and incubated with 300 nM 4',6-diamidino-2-phenylindole (DAPI) 10 min to stain the nuclei. The cells were then washed once with DPBS and once with DI water, and the chambers were removed. The slides were mounted, covered with glass coverslips, allowed to dry for a minimum of 2 h before sealing and stored at 4°C prior to visualization.

Images were acquired using a Nikon Eclipse TE2000 inverted confocal laser scanning microscope (Nikon Instruments, Melville, NY). Excitation and emission wavelengths for DAPI, OG/ AF488 and AF568 were 405/450, 488/515 and 543/605, respectively. Four Z-stacks were obtained for each treatment using the following microscope settings: 60× oil objective, 2× optical zoom, 60 μm pinhole and 512×512 pixel size. Z-stacks contained 41 0.5-mm slices to encompass the entire cell layer. Detector gains were set to be constant between samples to facilitate sample comparison.

Colocalization between G3.5-OG or Transferrin-AF488 with early endosomes and lysosomes was quantified using Volocity 3D Imaging software (Improvision, Lexing-

ton, MA). The extent of colocalization between the green and red channels ( $M_x$ ) was calculated by the software using the following equation:

$$M_x = \frac{\sum_i x_{i,coloc}}{\sum_i x_i}$$

where  $x_{i,coloc}$  is the value of voxel  $i$  of the overlapped red and green components, and  $x_i$  is the value of the green component.  $M_x$  is reported for each treatment as an average of the four regions. Transferrin-AF488 was used as an endocytosis control ligand to establish the validity of the assay methods for monitoring intracellular trafficking over time.

### Transepithelial Transport

Caco-2 cells were seeded at 80,000 cells/cm<sup>2</sup> onto polycarbonate 12-well Transwell filters of 0.4 μm mean pore size with 1.0 cm<sup>2</sup> surface area (Corning, Corning, NY). Caco-2 cells were maintained under standard incubation conditions where medium was changed every other day, and cells were used for transport experiments 21–25 days post-seeding. Prior to experiments, the transepithelial electrical resistance (TEER) of each monolayer was measured with an epithelial voltohmmeter (World Precision Instruments, Sarasota, FL). Monolayers with TEER > 600 Ωcm<sup>2</sup> were used for assays. Cell monolayers were washed with HBSS and then incubated in the presence of HBSS or endocytosis inhibitors for 1 h at 37°C. Inhibitors were used at concentrations that showed a minimum of 85% cell viability during the 2 h assay period (Table I). The solutions were removed, and G3.5-OG (10 μM) was added to the apical compartment in the presence of HBSS or endocytosis inhibitor, and the corresponding solution was added to the basolateral compartment. After incubating for 1 h, samples were taken from the basolateral compartment. Transport was quantified by measuring fluorescence in the basolateral compartment using a SpectraMax Gemini XS spectrofluorometer (Molecular Devices, Sunnyvale, CA) with excitation and emission wavelengths of 485 and 535 nm, respectively. Percent transport is reported comparing dendrimer transport in the presence of inhibitors to dendrimer transport in HBSS alone. The standard deviation for each reported value is calculated using propagation of error for the quotient of two experimentally determined values.

Lucifer yellow (LY) CH permeability was also monitored in the presence of HBSS and endocytosis inhibitors to ensure the integrity of the monolayers. LY apparent permeability was less than  $1 \times 10^{-6}$  for all conditions tested, which is within the accepted range of LY permeability for

differentiated monolayers (23). There was not a significant difference between LY permeability in the presence of HBSS or inhibitors, confirming that endocytosis inhibitors do not affect tight junctional integrity (data not shown).

### Caco-2 Monolayer Visualization and Occludin Staining

After acquisition of samples for transport assays, Caco-2 cell monolayers were prepared for visualization by confocal microscopy. In particular, Caco-2 cell monolayers treated with G3.5-OG or HBSS in buffer or in the presence of dynasore were analyzed for occludin accessibility. The monolayers were washed twice with ice-cold PBS, fixed, permeabilized and blocked by the same procedures used in the immunofluorescence studies (see section “Colocalization and Intracellular Trafficking” above). Subsequently, monolayers were treated with mouse anti-occludin (2 µg/ml) overnight at 4°C. The next day, monolayers were washed twice with blocking solution and incubated with the same solution for 30 min. Alexa Fluor 568 goat anti-mouse IgG (1:400) was added in blocking solution for 1 h. The cells were then washed and stained with DAPI. The membranes were carefully excised from the Transwell supports using a scalpel, mounted on glass slides, covered with a glass coverslip and then sealed with clear nail polish. Slides were stored at 4°C prior to visualization.

Images were acquired using a Nikon Eclipse TE2000 inverted microscope using the same settings as described above (“Colocalization and Intracellular Trafficking”). To visualize the G3.5 dendrimer interaction with the cell monolayer, Z-stacks were obtained with 51 0.5 µm slices using red, green and blue channels. To quantify occludin staining, four z-stacks were obtained per region, and only the red channel was used. Images were processed using Volocity software. Red voxels, corresponding to occludin staining, were quantified by thresholding the intensity between 20% and 100%. The number of red voxels was quantified for four z-stacks in each region. Results are reported as mean ± standard deviation, and statistical significance was determined by a one-way analysis of variance with Bonferroni post-hoc correction.

## RESULTS

### Cytotoxicity of Endocytosis Inhibitors

Five endocytosis inhibitors were chosen to examine the pathways of cellular uptake and transepithelial transport of G3.5 PAMAM dendrimers. Before initiating uptake and transport studies, Caco-2 cell viability during the 2 h assay time was confirmed in the presence of these inhibitors,

whose concentrations were chosen based on literature-reported values (20–22). Inhibitors included chemicals known to prevent clathrin-mediated endocytosis (phenylarsine oxide (1–20 µM); monodansyl cadaverine (100–300 µM)), caveolin-mediated endocytosis (filipin (1–4 µM); genistein (100–300 µM)) and dynamin-dependent endocytosis (dynasore (40–80 µM)). We have shown previously that G3.5 dendrimers do not cause a reduction in Caco-2 cell viability up to 100 µM (19). Since the maximal dendrimer concentration used in this work was 25 µM, toxicity due to the dendrimers was not a concern.

Short-term cytotoxicity of endocytosis inhibitors was assessed by the WST-1 cell viability assay at five different concentrations in the reported range of each inhibitor (Table I). Eighty-five percent cell viability was chosen as the minimum allowable for use in uptake and transport assays. Monodansyl cadaverine and filipin did not show appreciable toxicity at any concentration tested and were used at their maximum reported concentrations of 300 µM and 4 µM, respectively. Phenylarsine oxide and genistein showed significant toxicity and were used at their lowest effective concentrations. Dynasore showed increasing toxicity over the range of concentrations tested, with the most acceptable (i.e. >85% viability) toxicity profile at 50 µM (Table I).

### Cellular Uptake of G3.5-OG Dendrimers in the Presence of Endocytosis Inhibitors

As chemical inhibitors have varied effectiveness in different cell lines and can be somewhat non-specific, we took a multi-pronged approach, selecting one inhibitor for the general process of dynamin-dependent endocytosis and two inhibitors for distinct clathrin- and caveolin-mediated processes. In addition, we monitored the cellular uptake of transferrin and cholera toxin B, control ligands for clathrin- and caveolin-mediated endocytosis, respectively, to determine the efficacy and specificity of the selected inhibitors. Dynasore was used to block vesicular endocytosis by selectively inhibiting dynamin 1 and dynamin 2 GTPases, which are responsible for vesicle scission during both clathrin- and caveolin-mediated endocytosis (21). Monodansyl cadaverine and phenylarsine oxide were used to block clathrin-mediated endocytosis. Monodansyl cadaverine is known to stabilize clathrin-coated pits on the cell membrane, thereby preventing internalization (24). Phenylarsine oxide has also been shown to inhibit clathrin endocytosis at low micromolar concentrations, but its mechanism is unknown (25, 26). Filipin and genistein were selected to inhibit caveolin-mediated endocytosis. Filipin binds cholesterol and has been shown to disrupt caveolae-mediated endocytic pathways (27). Genistein inhibits protein tyrosine kinases and, amongst other effects, was

shown to block internalization by caveolae (28). The percent uptake relative to buffer control was calculated for G3.5 and control ligands in the presence of five endocytosis inhibitors (Table II).

G3.5 PAMAM dendrimers show reduction in cellular uptake in the presence of all endocytosis inhibitors tested, suggesting the involvement of both clathrin- and caveolin-mediated endocytosis pathways in dendrimer cellular uptake. As expected, dendrimers showed the greatest reduction in uptake in the presence of dynasore, a selective chemical inhibitor of dynamin, a protein integral to the hallmark event of vesicle pinching from the plasma membrane during receptor-mediated endocytosis. The significant decrease in uptake of dendrimers and control ligands in the presence of dynasore confirms the endocytosis of G3.5 PAMAM dendrimers by dynamin-dependent pathways. Dendrimers showed decreased uptake in the presence of both clathrin inhibitors, with a greater decrease seen in the presence of monodansyl cadaverine. Transferrin uptake was not reduced in the presence of phenylarsine oxide, indicating that this is not an effective clathrin-endocytosis inhibitor in Caco-2 cells at the concentration used, and the decrease in dendrimer uptake may be due to a non-specific effect. Alternatively, dendrimer trafficking may be more sensitive to phenylarsine oxide compared to transferrin and cholera toxin B, which are affected only at higher phenylarsine oxide concentrations. In contrast, transferrin shows reduced uptake in the presence of monodansyl cadaverine, illustrating the efficacy of monodansyl cadaverine in Caco-2 cells. Cholera toxin B also shows reduced uptake in the presence of monodansyl cadaverine, but this decrease in uptake was expected since cholera toxin B can be endocytosed by clathrin- and caveolin-mediated pathways in Caco-2 cells (29). Dendrimers also showed reduced uptake in the presence of both caveolin inhibitors, markedly seen with genistein; however, filipin did not reduce uptake of cholera toxin B, and this may represent a cell-specific effect. While genistein reduces the uptake of transferrin, it reduces the uptake of cholera toxin B to a much larger extent, making it an effective and relatively specific inhibitor of caveolin-mediated endocytosis. The most effective and specific inhibitors (monodansyl

cadaverine, genistein and dynasore) were chosen for further investigation in transport assays.

### Intracellular Trafficking

In addition to determining the mechanism of dendrimer uptake, we investigated the intracellular trafficking of G3.5 PAMAM dendrimers in Caco-2 cells. Dendrimers colocalized with early endosomes (EEA-1) and lysosomes (LAMP-1) over time (Fig. 1A). Transferrin trafficking (Fig. 1B), which has been well-characterized in this cell line, was used as a control for the study (17). Five minutes after incubation, dendrimers showed initial localization in the early endosomes and lysosomes. By 15 min, however, they showed increasing localization in the lysosomes, indicating quick trafficking to these cellular compartments. Interestingly, at 30 min, the level of accumulation in the lysosomes remained unchanged, while their presence in endosomes increased. This suggests that the trafficking pathway was saturated, causing dendrimer retention in early endosomes once lysosomes were occupied. In contrast, transferrin showed almost constant presence in the early endosomes with increasing presence in the lysosomes over time. This is typical of transferrin, a classical ligand for clathrin-mediated endocytosis, known to accumulate in the early endosomes, confirming the validity of the assay methods.

### Transepithelial Transport of G3.5-OG Dendrimers

Transepithelial transport of G3.5-OG dendrimers was monitored in the presence of endocytosis inhibitors at 4°C and compared to transport in buffer at 37°C (Fig. 2).

Transport of PAMAM G3.5 was significantly reduced at 4°C, illustrating strong energy dependence. Similar to Caco-2 uptake studies, transport was also reduced in the presence of dynasore and monodansyl cadaverine, indicating the importance of dynamin-dependent and clathrin-mediated endocytosis mechanisms in transepithelial transport. However, contrary to its effect on cellular uptake of dendrimers (Table II), genistein does not significantly impact dendrimer transport across Caco-2 monolayers, suggesting

**Table II** Percent Uptake of G3.5-OG Dendrimers and Control Ligands in Caco-2 Cells in the Presence of Endocytosis Inhibitors. Results are Reported as Mean  $\pm$  Standard Deviation with  $n = 2$

Endocytosis inhibitors		Percent uptake		
		G3.5	Transferrin	Cholera toxin B
Clathrin Inhibiting	Phenylarsine Oxide (PAO)	84.4 $\pm$ 0.6%	112.3 $\pm$ 1.5%	100.5 $\pm$ 4.0%
	Monodansyl Cadaverine (MDC)	57.8 $\pm$ 2.1%	65.6 $\pm$ 2.5%	61.8 $\pm$ 5.1%
Caveolin Inhibiting	Filipin (FIL)	81.0 $\pm$ 0.2%	110.2 $\pm$ 0.1%	114.4 $\pm$ 3.4%
	Genistein (GEN)	22.4 $\pm$ 0.7%	69.8 $\pm$ 2.4%	20.4 $\pm$ 0.7%
Dynamin Inhibiting	Dynasore (DYN)	20.4 $\pm$ 3.5%	15.0 $\pm$ 2.7%	57.1 $\pm$ 19.6%

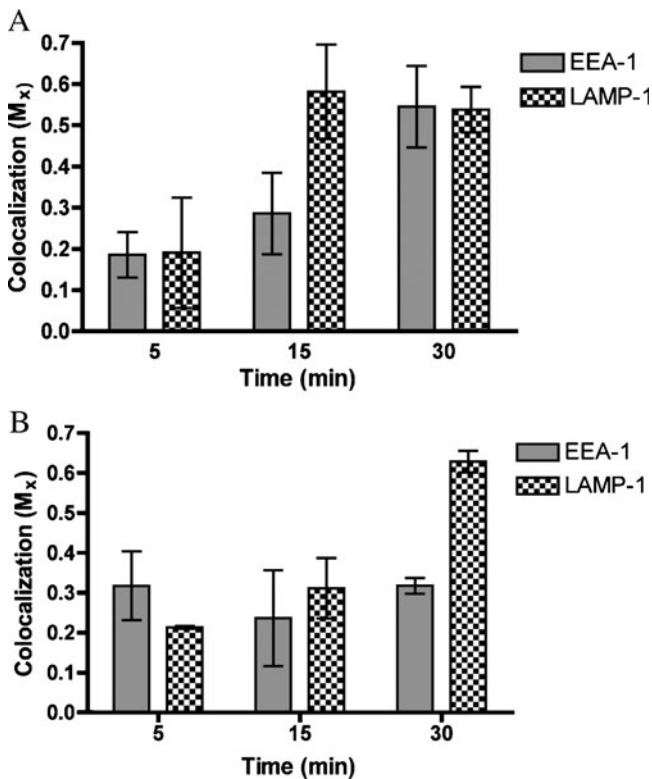


**Fig. 1** Intracellular trafficking of G3.5-OG dendrimers (**A**) and Transferrin (**B**) over time in Caco-2 Cells. Colocalization (M<sub>x</sub>) with early endosomes (EEA-1) and lysosomes (LAMP-1) is shown. Results are reported as mean  $\pm$  standard deviation ( $n=4$ ).

that caveolin-mediated endocytosis may not play a significant role in this process. It has been suggested that fully differentiated Caco-2 cells lack caveolae (29), opening the possibility that, while caveolae play an important role in dendrimer endocytosis in undifferentiated Caco-2 cells, they are less important in dendrimer transepithelial transport because of their lower expression in differentiated enterocytes.

### Visualization of G3.5-OG Dendrimer Interaction with Caco-2 Cell Monolayers

After cell monolayers were used for transport assays, they were fixed and stained for occludin and nuclear DNA. By excising the stained membranes from the transwell supports, we were able to visualize the dendrimer interacting with differentiated Caco-2 cell monolayers. Although there have been many studies documenting dendrimer interaction with Caco-2 cells grown on microscope slides (17), this is the first to show interaction with fully differentiated and confluent monolayers. Fig. 3 shows a representative image of the cell monolayer. The nuclear staining was omitted from Fig. 3B to allow for easier visualization of the dendrimer and tight junctions. In both figures, dendrimer staining is observed inside the confluent cells, confirming

internalization. In addition, there are punctate regions strongly resembling vesicles (circled in Fig. 3B), which confirm the involvement of vesicular endocytosis in dendrimer transepithelial transport. Finally, dendrimers cannot be detected in the nuclear region of the cell, confirming their localization in the cell interior and without further trafficking into the cell nucleus. These images serve as complementary evidence of the importance of the trans-cellular pathway in dendrimer transport.

### Cells Treated with Dynasore Do Not Show Increased Occludin Staining in Presence of Dendrimers

Increased occludin staining is a well-established indicator for tight junctional opening in Caco-2 cell monolayers and has shown strong correlation with reduction in TEER and increase in paracellular marker permeability (30). Previous studies have shown that monolayers treated with dendrimers showed increased occludin accessibility relative to cells treated with HBSS alone, indicating that dendrimers open tight junctions (4, 19). We examined occludin accessibility in Caco-2 cell monolayers treated with dendrimers or HBSS in the presence of dynasore or buffer alone (Figs. 4 and 5). In cells treated with buffer, dendrimers significantly increased occludin staining relative to untreated cells, indicating tight junction opening (Fig. 4A,B). In contrast, in cells treated with dynasore, no difference could be detected in occludin staining between cells treated with dendrimers or dynasore alone (Fig. 4C,D). This illustrates that dendrimers were unable to open tight junctions in cells where dynamin-dependent endocytosis was inhibited, suggesting that dendrimers must first be internalized to modulate cellular tight junctions.

Two major mechanisms have been established for opening tight junctions: depletion of divalent cations and disruption of intracellular tight junctional components. Disodium ethylenediaminetetraacetate, a calcium chelator,

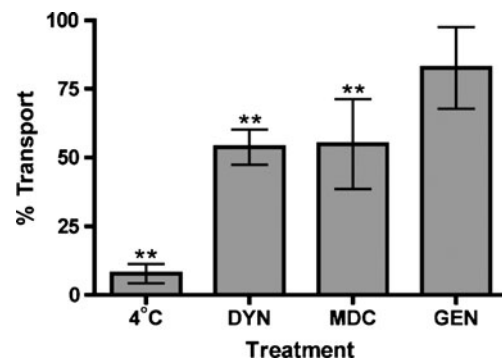
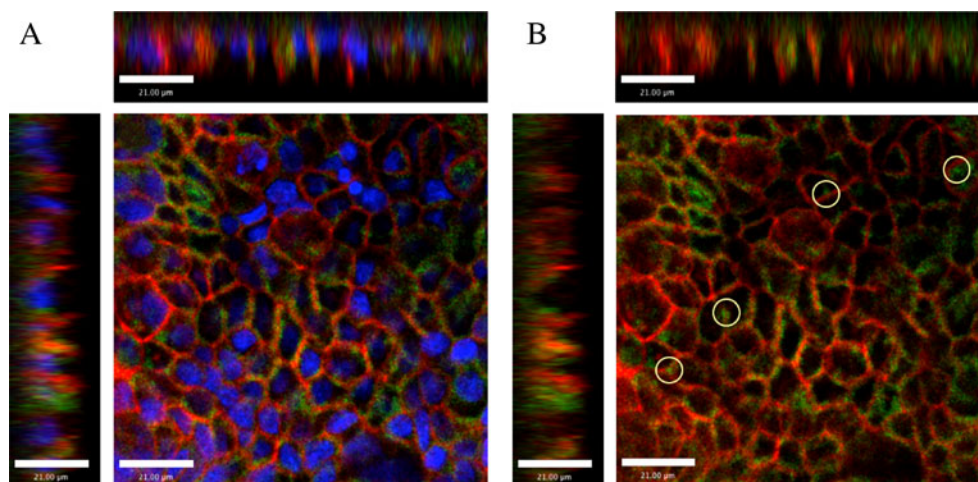


**Fig. 2** Percent transport of G3.5-OG dendrimers across Caco-2 monolayers in the presence of endocytosis inhibitors or at 4°C. Mean  $\pm$  standard deviation ( $n=4$ ). \*\* indicates a significant difference ( $p<0.01$ ) from 100% transport (buffer alone).

**Fig. 3** Visualization of G3.5-OG dendrimer interaction with Caco-2 monolayers. Dendrimers are localized inside cell monolayers but avoid the nucleus (**A**), and small vesicles of G3.5 dendrimers (circled) can be seen interacting with cells (**B**). Scale bar = 21  $\mu\text{m}$ .

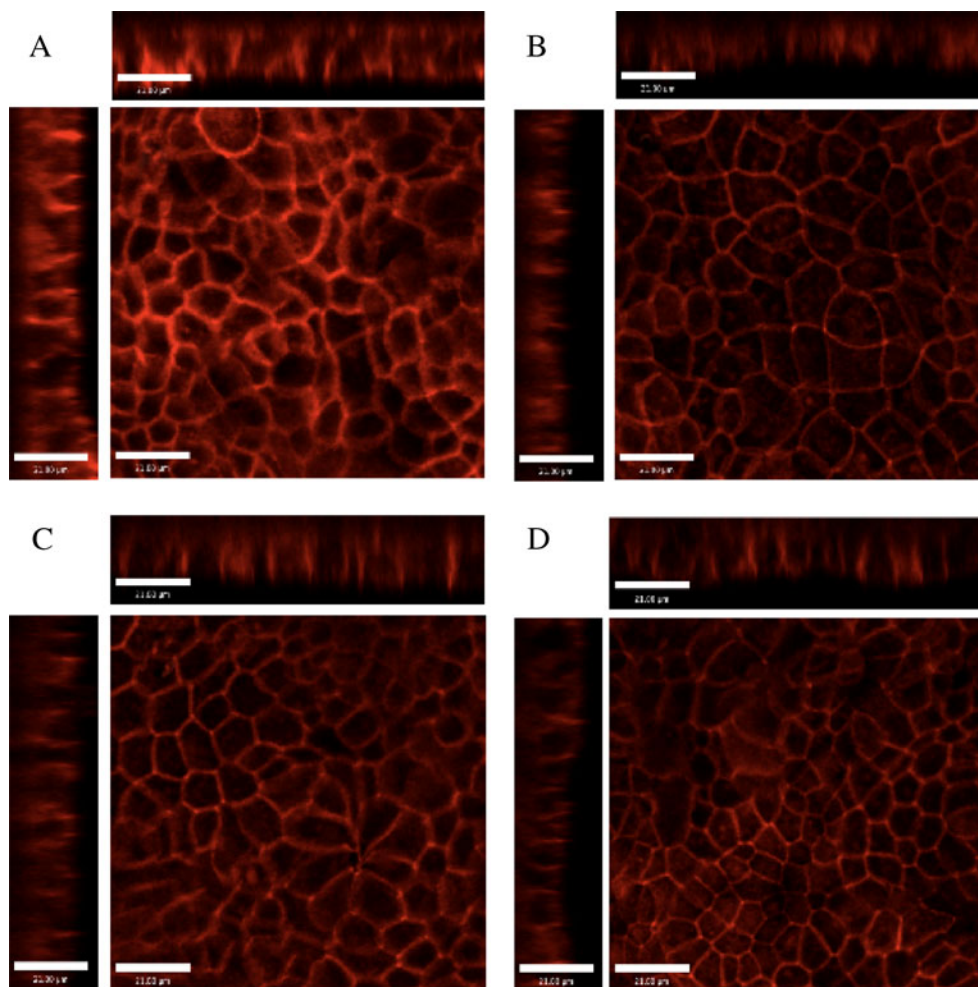


and polyoxyethylene, a surfactant, both lower extracellular calcium levels, causing dissociation of tight junctions (31). Other compounds, such as sodium caprate, increase tight junctional opening by initiating a biochemical-signaling cascade which results in the contraction of actin microfilaments, effectively dilating the intracellular tight junctions

(31). While it is possible that dendrimers interact with the tight junctions in multiple ways, it is clear that prevention of dendrimer endocytosis reduces both transcellular and paracellular transport, suggesting that dendrimer endocytosis is at least in part responsible for tight junction modulation. Dendrimers are most likely acting on intracel-

**Fig. 4** Occludin staining in the presence and absence of G3.5-OG dendrimers in Caco-2 cells treated with HBSS or Dynasore.

**A** G3.5/ HBSS, **B** HBSS only **C** G3.5/Dynasore and **D** Dynasore only. Main panels illustrate the xy plane; horizontal bars illustrate the xz plane; vertical bars illustrate the yz plane. Scale bars equal 21  $\mu\text{m}$ .





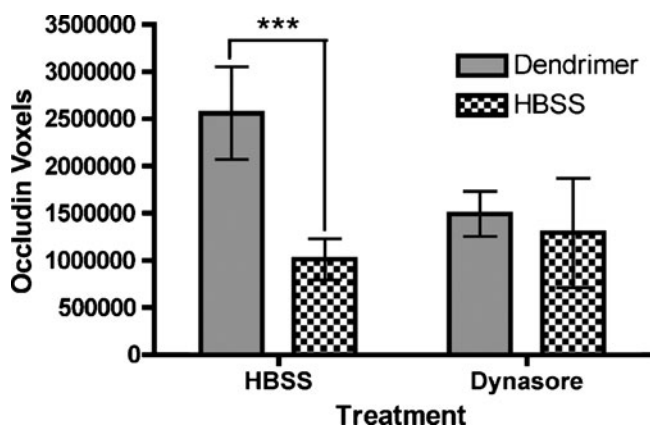


**Fig. 5** Quantification of occludin staining. Cells treated with G3.5-OG dendrimers in the presence of HBSS show a significant increase in occludin staining from untreated cells. (\*\*\*) indicates  $p < 0.001$ . Cells treated with dendrimer in the presence of dynasore do not show a significant change in occludin staining relative to the control. Results are reported as mean  $\pm$  standard deviation with  $n = 4$ .

lular cytoskeleton components to induce tight junction opening.

## DISCUSSION

PAMAM dendrimers have shown promise as oral drug delivery carriers due to their ability to translocate across the epithelial layer of the gut, taking poorly bioavailable drug cargo in tow (14). While many studies have suggested that dendrimers transiently open tight junctions and are transported through the intestinal barrier by transcellular and paracellular pathways (5, 10, 16), the details of these processes are poorly understood. In order to design dendrimers as oral drug delivery carriers, it is critical to know the detailed mechanisms of their cellular entry,

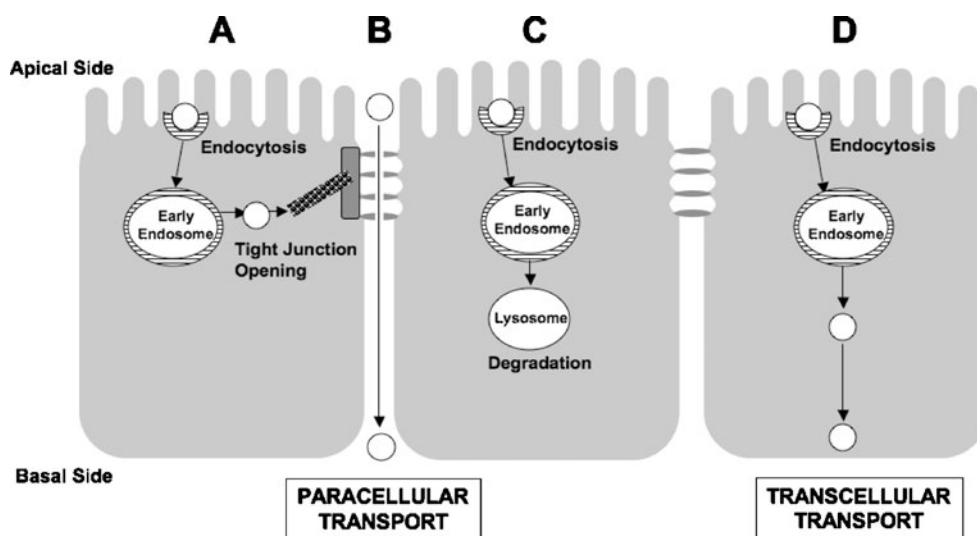
trafficking, transport and interaction with cellular tight junctions. In this work, we have uncovered some of the details of anionic dendrimer transport, which can have significant implications for oral drug delivery.

Caco-2 cellular uptake of G3.5 dendrimers was found to occur primarily through dynamin-dependent endocytosis pathways, specifically clathrin- and caveolin-mediated endocytosis. Previous reports have suggested the involvement of clathrin in dendrimer endocytosis (17). The present study confirms, for the first time, the involvement of caveolin-mediated endocytosis in dendrimer internalization. This suggests that dendrimers are not relegated to a single means of cellular entry, but instead take advantage of several specific endocytosis pathways. This has significant implications for drug delivery, as intracellular trafficking is largely dependent on initial pathway of cell entry. Therefore, it is to be expected that a portion of dendrimer dose applied to enterocytes will be trafficked to the lysosomes by the clathrin-mediated endocytosis pathway, while the dendrimers that enter via the caveolae may end up in the cell cytosol, allowing dendrimers to be targeted to either compartment depending on the desired effect.

Dendrimer transport across differentiated Caco-2 cell monolayers was found to be dependent on dynamin- and clathrin-mediated endocytosis, but independent of caveolin-mediated endocytosis. This result was expected, since fully differentiated Caco-2 cells lack caveolae. The differences between dendrimer transport across differentiated epithelial cells and uptake in undifferentiated cells can be exploited potentially by drug delivery strategies that aim to specifically target cancer cells while simultaneously avoiding intestinal cells by designing linkers that would be cleaved in caveolae-mediated transport pathways.

Intracellular trafficking studies shed further light on the environments that dendrimers encounter after cellular

**Fig. 6** Dendrimer transport across Caco-2 cell monolayers. Once endocytosed, dendrimers can interact with tight junctions (A), allowing for paracellular transport (B), or they can be degraded by the lysosomes (C) or transcytosed (D).



internalization. Kitchens and co-workers (17) examined G1.5 and G2 dendrimer colocalization with endosomal and lysosomal markers in Caco-2 cells and reported that dendrimers show constant presence in the early endosomes at 20 and 60 min, with time-dependent trafficking to the lysosomes. In this study G3.5 dendrimers were found to localize in the early endosomes and lysosomes after 5 min, displayed fast trafficking to the lysosomes after 15 min and increased endosomal and lysosomal accumulation at 30 min, likely due to pathway saturation. Often, drugs are conjugated to dendrimers via pH-sensitive linkers that are cleaved in the acidic environment of mature endosomes or peptide linkers that are cleaved by lysosomal enzymes such as cathepsin B (32). These intracellular trafficking studies corroborate the validity of such strategies, as dendrimers can be found in both environments following cellular internalization. Cleavage of pH-sensitive linkers in the endosomes may be promising, as dendrimers are shown to accumulate in these compartments over time. Knowledge of the cellular uptake and intracellular trafficking pathways of dendrimers can have significant impacts on designing them for use as drug delivery vehicles. In the context of oral drug delivery, knowledge of subcellular localization in intestinal cells can enable design of conjugates that are robust in these compartments and absorbed intact to the blood-stream.

One of the most intriguing attributes of PAMAM dendrimers is that within a specified size and charge window, they have been shown to catalyze their own transport via the paracellular pathway (5). Previous reports have shown that dendrimers cause decreases in TEER, increases in paracellular marker flux (e.g. mannitol) and increased occludin accessibility in Caco-2 cells, confirming that dendrimers open tight junctions (5–7). However, the mechanism behind this phenomenon remained largely elusive. In this study, we examined the role of dendrimer cellular internalization in tight junction opening by monitoring the effects of dendrimers on confluent monolayers in buffer or in the presence of dynasore. While dendrimers were able to open tight junctions in the presence of buffer alone, they could not do so in the presence of dynasore, suggesting that dendrimer internalization is requisite for tight junction opening. This has significant implications for oral delivery using dendrimers because it shows that tight junction opening is at least in part modulated by dendrimers *within* the cells. Whether affecting tight junctional structures from the apical environment *outside* the cells by dendrimers also plays a role remains to be examined. Therefore, this mechanism (opening tight junction by internalization) results in temporary tight junction opening, which is consistent with our previous reports that TEER returns to pre-treatment values after 24 h (33). Taken together, these data establish that dendrimers can be used

safely as oral drug carriers or penetration enhancers since, depending on generation, concentration and incubation time, their effects on tight junctions can be transient, not permanent. Fig. 6 summarizes some of the possible G3.5 transport pathways across Caco-2 cell monolayers.

## CONCLUSION

In this work, we report the detailed mechanisms of cellular uptake, intracellular trafficking, transport and tight junction modulation of G3.5 PAMAM dendrimers in Caco-2 cells. We find that G3.5 PAMAM dendrimers enter undifferentiated Caco-2 cells by clathrin-, caveolin-, and dynamin-dependent pathways but that their transepithelial transport across confluent monolayers is governed by clathrin- and dynamin-dependent pathways only. Dendrimers are quickly trafficked to the lysosomes, but show increased endosomal accumulation once the lysosomal compartments become saturated. Finally, it is demonstrated that dendrimer endocytosis promotes tight junction opening, illustrating the interconnected nature of the transcellular and paracellular pathways in dendrimer transepithelial transport. Knowledge of detailed mechanisms of dendrimer cellular uptake, intracellular and transepithelial transport will assist in the design of PAMAM dendrimer-based oral drug delivery strategies by providing appropriate linker chemistry consistent with transepithelial transport and cellular trafficking pathways.

## ACKNOWLEDGEMENTS

Financial Support was provided by a National Science Foundation Graduate Research Fellowship and the Fischell Fellowship in Bioengineering to D. Goldberg, and NIH R01EB07470. Flow cytometry analysis was performed at the Flow Cytometry Core Laboratory, Center for Vaccine Development, School of Medicine, University of Maryland, Baltimore.

## REFERENCES

1. Tomalia DA. Birth of a new macromolecular architecture: dendrimers as quantized building blocks for nanoscale synthetic polymer chemistry. *Prog Polym Sci.* 2005;30:294–324.
2. Tomalia DA, Reyna LA, Svenson S. Dendrimers as multi-purpose nanodevices for oncology drug delivery and diagnostic imaging. *Biochem Soc Trans.* 2007;35:61–7.
3. Kolhatkar R, Sweet D, Ghandehari H. Functionalized dendrimers as nanoscale drug carriers. In: Torchilin V, editor. *Multifunctional pharmaceutical nanocarriers.* New York: Springer; 2008. p. 201–32.
4. Kitchens KM, Kolhatkar RB, Swaan PW, Eddington ND, Ghandehari H. Transport of poly(amidoamine) dendrimers across

- caco-2 cell monolayers: influence of size, charge and fluorescent labeling. *Pharm Res.* 2006;23:2818–26.
5. Kitchens KM, El-Sayed ME, Ghandehari H. Transepithelial and endothelial transport of poly (amidoamine) dendrimers. *Adv Drug Delivery Rev.* 2005;57:2163–76.
  6. El-Sayed M, Ginski M, Rhodes C, Ghandehari H. Transepithelial transport of poly(amidoamine) dendrimers across Caco-2 cell monolayers. *J Controlled Release.* 2002;81:355–65.
  7. El-Sayed M, Ginski M, Rhodes C, Ghandehari H. Influence of surface chemistry of poly (amidoamine) dendrimers on Caco-2 cell monolayers. *J Bioact Compat Polym.* 2003;18:7–22.
  8. Jevprasesphant R, Penny J, Jalal R, Attwood D, McKeown NB, D'Emanuele A. The influence of surface modification on the cytotoxicity of PAMAM dendrimers. *Int J Pharm.* 2003;252:263–6.
  9. Jevprasesphant R, Penny J, Attwood D, McKeown NB, D'Emanuele A. Engineering of dendrimer surfaces to enhance trans-epithelial transport and reduce cytotoxicity. *Pharm Res.* 2003;20:1543–50.
  10. Jevprasesphant R, Penny J, Attwood D, D'Emanuele A. Transport of dendrimer nanocarriers through epithelial cells via the transcellular route. *J Controlled Release.* 2004;97:259–67.
  11. Najlah M, Freeman S, Attwood D, D'Emanuele A. *In vitro* evaluation of dendrimer prodrugs for oral drug delivery. *Int J Pharm.* 2007;336:183–90.
  12. D'Emanuele A, Jevprasesphant R, Penny J, Attwood D. The use of a dendrimer-propranolol prodrug to bypass efflux transporters and enhance oral bioavailability. *J Controlled Release.* 2004;95:447–53.
  13. Ke W, Zhao Y, Huang R, Jiang C, Pei Y. Enhanced oral bioavailability of doxorubicin in a dendrimer drug delivery system. *J Pharm Sci.* 2008;97:2208–16.
  14. Kolhatkar RB, Swaan PW, Ghandehari H. Potential oral delivery of 7-ethyl-10-hydroxy-camptothecin (sn-38) using poly(amidoamine) dendrimers. *Pharm Res.* 2008;25:1723–9.
  15. Le Lay K, Myon E, Hill S, Riou-Franca L, Scott D, Sidhu M *et al.* Comparative cost-minimisation of oral and intravenous chemotherapy for first-line treatment of non-small cell lung cancer in the UK NHS system. *Eur J Health Econ.* 2007;8:145–51.
  16. Kitchens KM, Kolhatkar RB, Swaan PW, Ghandehari H. Endocytosis inhibitors prevent poly(amidoamine) dendrimer internalization and permeability across caco-2 cells. *Mol Pharmaceutics.* 2008;5:364–9.
  17. Kitchens K, Foraker A, Kolhatkar R, Swaan P, Ghandehari H. Endocytosis and interaction of poly (amidoamine) dendrimers with Caco-2 cells. *Pharm Res.* 2007;24:2138–45.
  18. Wiwattanapatapee R, Carreño-Gómez B, Malik N, Duncan R. Anionic PAMAM dendrimers rapidly cross adult rat intestine *in vitro*: a potential oral delivery system? *Pharm Res.* 2000;17:991–8.
  19. Sweet D, Kolhatkar R, Ray A, Swaan P, Ghandehari H. Transepithelial transport of pegylated anionic poly(amidoamine) dendrimers: implications for oral drug delivery. *J Controlled Release.* 2009;138:78–85.
  20. Ivanov A. Pharmacological inhibition of endocytic pathways: Is it specific enough to be useful? Exocytosis and endocytosis: Humana Press; 2008. p. 15–33.
  21. Macia E, Ehrlich M, Massol R, Boucrot E, Brunner C, Kirchhausen T. Dynasore, a cell-permeable inhibitor of dynamin. *Dev Cell.* 2006;10:839–50.
  22. Lühmann T, Rimann M, Bittermann AG, Hall H. Cellular uptake and intracellular pathways of PLL-PEG-DNA nanoparticles. *Bioconjugate Chem.* 2008;19:1907–16.
  23. Inokuchi H, Takei T, Aikawa K, Shimizu M. The effect of hyperosmosis on paracellular permeability in Caco-2 cell monolayers. *Biosci Biotechnol Biochem.* 2009;73:328–34.
  24. Phonphok Y, Rosenthal KS. Stabilization of clathrin coated vesicles by amantadine, tromantadine and other hydrophobic amines. *FEBS Lett.* 1991;281:188–90.
  25. Gibson AE, Noel RJ, Herlihy JT, Ward WF. Phenylarsine oxide inhibition of endocytosis: effects on asialofetuin internalization. *AJP-Cell Physiology.* 1989;257:C182–4.
  26. Sato K, Nagai J, Mitsui N, Ryoko Y, Takano M. Effects of endocytosis inhibitors on internalization of human IgG by Caco-2 human intestinal epithelial cells. *Life Sci.* 2030;85:800–7.
  27. Ma Z, Lim L-Y. Uptake of chitosan and associated insulin in Caco-2 cell monolayers: a comparison between chitosan molecules and chitosan nanoparticles. *Pharm Res.* 2003;20:1812–9.
  28. Van Hamme E, Dewerchin HL, Cornelissen E, Verhasselt B, Nauwynck HJ. Clathrin- and caveolae-independent entry of feline infectious peritonitis virus in monocytes depends on dynamin. *J Gen Virol.* 2008;89:2147–56.
  29. Torgersen ML, Skretting G, van Deurs B, Sandvig K. Internalization of cholera toxin by different endocytic mechanisms. *J Cell Sci.* 2001;114:3737–47.
  30. Roger E, Lagarce F, Garcion E, Benoit J-P. Lipid nanocarriers improve paclitaxel transport throughout human intestinal epithelial cells by using vesicle-mediated transcytosis. *J Controlled Release.* 2009;140:174–81.
  31. Kondoh M, Yagi K. Tight junction modulators: promising candidates for drug delivery. *Curr Med Chem.* 2007;14:2482–8.
  32. Kurtoglu Y, MM MK, Kannan S, RK RM. Drug release characteristics of PAMAM dendrimer-drug conjugates with different linkers. *Int J Pharm.* 2010;384:189–94.
  33. Kolhatkar RB, Kitchens KM, Swaan PW, Ghandehari H. Surface acetylation of polyamidoamine (PAMAM) dendrimers decreases cytotoxicity while maintaining membrane permeability. *Bioconjugate Chem.* 2007;18:2054–60.